

000 001 002 003 004 005 006 007 008 009 010 CTQWFORMER: A CTQW-BASED TRANSFORMER FOR GRAPH CLASSIFICATION

005 **Anonymous authors**

006 Paper under double-blind review

ABSTRACT

011 Graph Neural Networks (GNN) and Transformer-based architectures have
012 achieved remarkable progress in graph learning, yet they still struggle to capture
013 both global structural dependencies and model the dynamic information propa-
014 gation. In this paper, we propose CTQWformer, a hybrid graph learning frame-
015 work that integrates continuous-time quantum walks (CTQW) with GNN. CTQW-
016 former employs a trainable Hamiltonian that fuses graph topology and node fea-
017 tures, enabling physically grounded modeling of quantum walk dynamics that cap-
018 tures rich and intricate graph structure information. The extracted CTQW-based
019 representations are incorporated into two complementary modules: (i) a Graph
020 Transformer module that embeds final-time propagation probabilities as structural
021 biases in self-attention mechanism, and (ii) a Graph Recurrent Module that cap-
022 tures temporal evolution patterns with bidirectional recurrent networks. Extensive
023 experiments on benchmark graph classification datasets demonstrate that CTQW-
024 former outperforms graph kernel and GNN-based methods, demonstrating the po-
025 tential of integrating quantum dynamics into trainable deep learning frameworks
026 for graph representation learning. To the best of our knowledge, CTQWformer is
027 the first hybrid CTQW-based Transformer, integrating CTQW-derived structural
028 bias with temporal evolution modeling to advance graph learning.

029 1 INTRODUCTION

030
031 Graph-structure data is ubiquitous, and widely used in various domains including social networks,
032 bioinformatics, computer vision. Graph Neural Networks (GNNs) have emerged as a powerful tool
033 for graph learning tasks over graph-structure data, primarily through message passing and neigh-
034 borhood aggregation mechanisms Wu et al. (2020). Various GNN models have been developed
035 to address different node-level or graph-level tasks. Among these, graph classification constitutes
036 a fundamental graph-level problem that critically depends on accurately modeling the underlying
037 topological structure and the inter-node relationships within graphs.

038 Inspired by the successful application of Transformers in various domains, researchers have explored
039 using Transformers framework for graph learning, owing to their parallel computation efficiency
040 and strong capability in modeling long-range dependencies. These efforts include directly model-
041 ing graph structure or incorporating with GNNs to enhance the performance of various tasks. For
042 instance, Graph Transformer Networks is proposed to learn new graph structures via attention-like
043 modules and then apply conventional GNNs in node classification task Yun et al. (2019). Simi-
044 larly, Ying et al proposed Graphomer Ying et al. (2021), which apply Transformer architectures
045 to graph data by incorporating different structural encodings into the attention mechanism in graph
046 classification task.

047 However, traditional GNNs are often limited by their local receptive fields and suffer from issues
048 such as over-smoothing problem and inability to capture long-range dependencies among nodes
049 Corso et al. (2024). Despite the integration of global attention mechanisms and structural biases,
050 Transformer-based GNN models often struggle to effectively capture the intrinsic topological struc-
051 ture and global dependencies inherent in graph data.

052 In parallel, quantum computing provides a novel computational paradigm via its natural capability
053 for parallel information processing. As the quantum analogue of classical random walks, quantum
walks have emerged as a powerful framework for graph learning, owing to their dynamic evolution

on graphs that captures rich and intricate structural information Bai et al. (2015). Specifically, governed by the Schrödinger equation, continuous-time quantum walks (CTQW) offer a powerful and physically grounded way to model graph structure through its dynamical evolution. The constructive and destructive interference effects inherent in CTQW lead to more complex dynamic behaviors in the diffusion process, reflecting local and global properties of graphs, providing insightful structural information beyond its classical features Aharonov et al. (2001).

In this paper, we propose a hybrid graph learning framework, CTQWformer, which integrates CTQW-based physical structural bias and temporal evolution into a unified framework for graph classification task. Our model consists of three core components: (1) The Quantum Walk Encoder (QWE) achieves the dynamical evolution of CTQW over graph structures by modeling node-wise propagation probabilities under different configurations within graph datasets, guided by a trainable Hamiltonian that integrates both underlying graph topology and node features. (2) The Quantum Walk-Graph Transformer (QWGT) module incorporates the final-time propagation probabilities as intrinsic physical structural biases to guide the attention mechanism in graph Transformer. (3) The Quantum Walk-Graph Recurrent (QWGR) module employs a bidirectional recurrent network to processes the dynamic temporal evolution of CTQW, capturing the temporal sequence of node-wise propagation probability among graph. Together, these modules enable CTQWformer to effectively integrate both static physical structural biases and dynamic temporal evolution patterns of CTQW on graphs for graph-level representation learning.

As a result, the contribution of the paper is summarized as follows. First, we design a parameterized Hamiltonian that incorporates both graph structure and node features, which makes the dynamic evolution of CTQW not only rely on the static graph structure, but adaptively capture the connections of node features. The mechanism allows the model to be more suitable for the downstream tasks such as attributed graph classification. Second, we propose the CTQWformer model, a hybrid graph learning framework based on CTQW for graph classification. Specifically, the QWE module implements a trainable CTQW guided by a learnable Hamiltonian that integrates both graph structure and node features, enabling the extraction of dynamical evolution information under various configurations on graphs. The QWGT module encodes static physical structure bias generated by CTQW into attention mechanism in graph Transformer. And the QWGR module utilize bidirectional recurrent neural network to process the dynamic evolution information of CTQW. Together, the proposed module is capable of capturing both static and dynamic evolution information of CTQW on graphs, providing richer information of graph structure and more discriminative representation for graph-level tasks. Third, experiments conducted on several benchmark graph classification datasets demonstrate the effectiveness of our model, achieving competitive performance compared to state-of-the-art methods.

2 RELATED WORKS

2.1 GRAPH LEARNING

Early approaches to graph learning primarily relied on graph kernel methods, which measure the similarity between graphs by mapping their structure information into a high dimensional Hilbert space Kriege et al. (2020). A wide range of graph kernels have been proposed, many of which fall under the R-convolution framework Haussler et al. (1999), graph similarity is computed by comparing substructures such as walks, subgraphs, and subtrees. Representative examples include the Graphlet kernel Shervashidze et al. (2009) and the Weisfeiler-Lehman subtree kernel Shervashidze et al. (2011). In addition, recent works have explored information-theoretic graph kernels, which measure graph similarity from the perspective of entropy. Several information-theoretic graph kernels have been proposed, such as JTQK Bai et al. (2014), QJSK Bai et al. (2015), HAQJSK Bai et al. (2024), and AERK Cui et al. (2023), all of which are defined based on CTQW and aim to capture both structural and dynamical properties of graphs from the perspective of entropy. These kernels demonstrate the effectiveness of quantum walks as a powerful and efficient tool for graph learning. Although effective in small-scale datasets, kernel methods often suffer from poor scalability and limited expressive power. Typically, a graph kernel is a semi-definite function defined as

$$k(G_1, G_2) = \langle \phi(G_1), \phi(G_2) \rangle \quad (1)$$

Where G_1 and G_2 are two graphs, $\phi(\cdot)$ denotes the mapping from the input space to a reproducing kernel Hilbert space, and $\langle \cdot, \cdot \rangle$ could be the inner product in the space.

In recent years, GNNs have become the dominant paradigm for graph learning Corso et al. (2024). GNNs learn node and graph representations via neighborhood aggregation mechanism, enabling message-passing across the graph. Typically, GNN perform neighborhood aggregation using spectral-based approaches such as GCN Kipf & Welling (2016), or spatial-based approaches such as GraphSAGE Hamilton et al. (2017) and GIN Xu et al. (2018). Specifically, GCN updates node features by linearly combining the normalized features of their neighbors. GraphSAGE samples a fixed-size set of neighbors and aggregates their features via functions such as mean, LSTM or pooling, enabling inductive learning on large-scale graphs. GIN is designed to achieve maximal expressive power among message-passing GNNs, matching the discriminative capacity of the Weisfeiler-Lehman graph isomorphism test. However, traditional GNNs struggle with long-range dependencies and often suffer from over-smoothing with the increasing depth of networks. Further, to address these limitations, inspired by the success of self-attention mechanism in natural language processing, graph Transformer models have been developed such as Graphomer Ying et al. (2021), GraphGPS Rampášek et al. (2022). However, these models still face challenges: their ability to explicitly model local interactions remains limited, and their interpretability is relatively weak. These drawbacks motivate our approach, which leverages physically grounded quantum walk dynamics to provide both richer local structural modeling and improved interpretability. Formally, the self-attention mechanism in the Transformer framework Vaswani et al. (2017) is defined as

$$\text{Attention}(Q, K, V) = \text{softmax}\left(\frac{QK^T}{\sqrt{d}}\right)V \quad (2)$$

Where $Q, K, V \in R^{n \times d}$ are the query, key and value matrices derived from the input features respectively. In graph Transformers the input features are node features or edge features, and d is the dimensionality scaling factor.

2.2 CONTINUOUS-TIME QUANTUM WALK

Recently, quantum walks, as a general framework for designing quantum algorithms in quantum computing, have demonstrated substantial potential in addressing a variety of graph learning tasks including graph classification Bai et al. (2015), node classification Yan et al. (2022) and link prediction Goldsmith et al. (2023).

Unlike classical random walks, quantum walks leverage superposition and interference to generate fundamentally different propagation behaviors. The dynamical evolution of quantum walks on graphs offers a distinctive perspective for capturing both structural and dynamical properties of graphs, such as probability distribution, spectral of density matrix and von Neumann entropy. Generally, there are two kinds of quantum walks: continuous-time quantum walks and discrete-time quantum walks (DTQW), both of which have demonstrated substantial potential in various graph learning algorithms including graph isomorphism, link prediction and graph kernels Kadian et al. (2021).

Motivated by GQWformer, which pioneers the integration of DTQW and graph Transformers in graph learning Yu et al. (2024). In this paper, we utilize CTQW as it does not require additional coin operators, resulting in more natural and analytically tractable dynamics. This coin-free and analytically tractable formulation not only reduces the effective Hilbert space, simplifies the evolution process but also enables a more expressive and physically grounded encoding of graph structures and node features. By employing a learnable Hamiltonian that fuses graph structure and node features, the trainable CTQW provides a more physically grounded and flexible framework for graph learning.

Specifically, for a graph $G = (V, E)$, $n = |V|$ denotes the number of nodes of the graph. In CTQW, the state space of the walker is a Hilbert space $H = \text{span}\{|1\rangle, |2\rangle, \dots, |n\rangle\}$, which is spanned by the position basis states corresponding to the vertices of the graph. The state of the walker is described by a complex vector $|\psi\rangle = [\alpha_1, \alpha_2, \dots, \alpha_n]$, where α_i denotes the probability amplitude at vertex i . As a result, the quantum state $|\psi(t)\rangle$ of CTQW at time t is described as a complex linear combination of these basis states over all vertices.

$$|\psi(t)\rangle = \sum_{v \in V} \alpha_v(t) |v\rangle \quad (3)$$

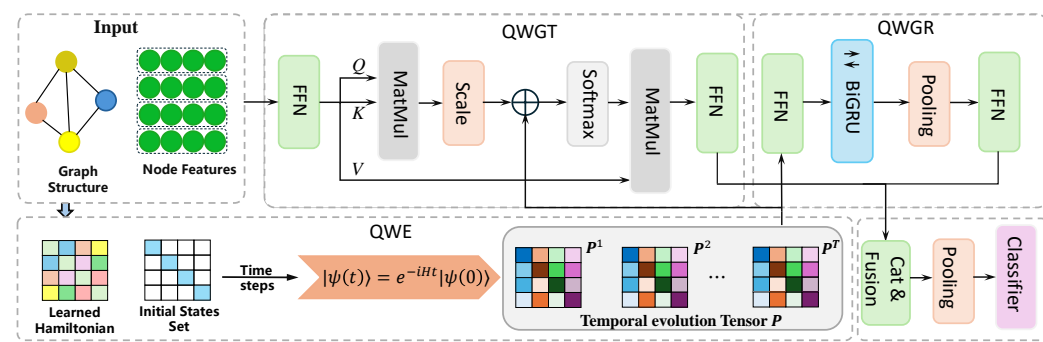


Figure 1: Illustration of the proposed CTQWformer model. The model integrates CTQW dynamics into graph learning via three core components: (1) QWE simulates trainable CTQW to encode graph structure and features into a time-evolution tensor; (2) QWGT uses final-time propagation probabilities as structural biases in a Transformer; (3) QWGR employs BiGRU to capture node-level temporal dynamics. QWGT and QWGR are fused per layer, enabling deep stacked learning. A global mean pooling and classifier produce the final graph-level prediction.

The equation satisfies $\sum_{v \in V} \alpha_v(t) \alpha_v^*(t) = 1$ for all nodes at any time t . $\alpha_v^*(t)$ is the complex conjugate of $\alpha_v(t)$. The time evolution of the quantum walker is governed by unitary operator $U(t) = e^{-iHt}$. Where i is imaginary unit, H is the Hamiltonian that encodes the graph structure, usually taken from the adjacency matrix A or Laplacian matrix $L = D - A$, where D is the degree matrix, in this paper, we adopt the Laplacian matrix. Finally, the dynamics of the system are described by the Schrödinger equation

$$i \frac{d}{dt} |\psi(t)\rangle = H |\psi(t)\rangle \quad (4)$$

Given initial state $|\psi(0)\rangle$ and time t , the state of walker is described as follow

$$|\psi(t)\rangle = U(t)|\psi(0)\rangle = e^{-iHt}|\psi(0)\rangle \quad (5)$$

After the state evolution, we perform a measurement to get the probability distribution of the walker over the graph at time t , the probability of the walker at node i is given by

$$p_i(t) = |\langle i | \psi(t) \rangle|^2 \quad (6)$$

Our work builds upon this line of research by integrating CTQW-based features into a trainable graph learning framework, allowing for joint learning of dynamics of CTQW and task-specific graph learning.

3 METHOD

3.1 THE OVERVIEW OF THE CTQWFORMER MODEL

Formally, given a graph dataset $\mathcal{G} = \{G_1, G_2, \dots, G_N\}$ where each graph G_i is associated with a graph label $y_i \in R$ and node features $X_i \in R^{n \times d}$, the goal of graph classification is to learn a function that maps an input graph to its corresponding label.

We propose CTQWformer, a novel architecture for graph classification that integrates both static and dynamic information derived from CTQW. The model combines a graph Transformer to capture physically grounded structural bias and a graph recurrent network to model the temporal evolution patterns embedded in the dynamics of CTQW. The proposed model consists of three main components. First, we perform CTQW on graphs to extract encoded information. A learnable Hamiltonian is constructed by integrating graph structure and node features making CTQW trainable and the model to be attribute-aware. Meanwhile, the dynamics evolution of CTQW captures non-local dependencies and global topological features embedded in the graphs. Finally, we perform measurement at discrete time steps $\{t_1, t_2, \dots, t_T\}$ to get CTQW evolution tensor $P \in R^{T \times n \times n}$ that

216 encodes the structural and dynamical information of the graphs. The tensor is used in two ways:
 217 (1) the final time step probability matrix P^T serves as a structural bias for the graph Transformer;
 218 (2) the full tensor P is passed to graph recurrent networks for temporal modeling. Second, we
 219 employ a graph Transformer that integrates CTQW-based information to capture structural depen-
 220 dencies. Specifically, extracted from evolution tensor P , the final time step probability matrix P^T
 221 is designed as a structural bias matrix within the self-attention mechanism to guide the learning of
 222 pairwise node interactions. Third, we employ graph recurrent networks based on bidirectional gated
 223 recurrent unit (BiGRU) to capture the temporal dynamics of CTQW. The evolution tensor P consists
 224 of a temporal sequence of node-pair probability matrices, from which we extract node-wise tempo-
 225 ral propagation probabilities from the diagonal elements of node-pair probability matrices, enabling
 226 the model to capture dynamic propagation patterns of individual nodes over time.
 227

228 We integrate the QWGT and QWGR modules into a unified layer, making the architecture suit-
 229 able for deep graph learning through multi-layer stacking. In each layer, the outputs derived from
 230 the QWGT module and the QWGR module are concatenated and passed through a fusion network
 231 that effectively combines the static physical structural bias and dynamic temporal evolution fea-
 232 tures to update node representations. Finally, after multiple stacked layers, a global mean pooling
 233 operation is applied on the resulting node embeddings to derive a graph-level representation. The
 234 representation is subsequently passed through a final classifier to perform graph-level prediction.
 235 The framework of the model is exhibited in Fig.1.
 236

237 3.2 THE QUANTUM WALK ENCODER

238 The core of our model lies in encoding CTQW-based static physical structural bias and dynamical
 239 evolution information into the graph representation. To achieve this, we first construct a trainable
 240 Hamiltonian that governs the dynamics of CTQW on the graph. This allows the quantum evolu-
 241 tion process to be optimized jointly with downstream tasks, making the model structure-aware and
 242 feature-aware.

243 Specifically, the Hamiltonian $H \in R^{n \times n}$ is designed to integrate both the graph topology and
 244 node features. Given a graph $G = (V, E)$ with n nodes and node features $X \in R^{n \times d}$, where
 245 d is the dimension of node features. We define a learnable Hamiltonian to construct a trainable
 246 CTQW, allowing the model to flexibly adjust to varying graph topologies and node features during
 247 the dynamical evolution process. For each edge $(i, j) \in E$, we concatenate the features of two
 248 incident nodes to form an edge feature vector

$$249 \quad e_{ij} = [x_i || x_j] \in R^{2d} \quad (7)$$

250 A two-layer perception with non-linear activation is applied to map the edge features into scalar
 251 edge weights.

$$252 \quad w_{ij} = \sigma(W_2 \cdot \phi(W_1 e_{ij})) \quad (8)$$

253 Where $\phi(\cdot)$ is ReLU nonlinear activation function and $\sigma(\cdot)$ denotes the sigmoid function to ensure
 254 the weights are bounded in [0,1]. These learned edge weights form a new weighted adjacency
 255 matrix. To ensure the Hermitian property required by the evolution operator, we get symmetrized
 256 matrix

$$257 \quad A_{sym} = \frac{1}{2} (A + A^T) \quad (9)$$

258 The final Hamiltonian is defined as a Laplacian matrix

$$259 \quad H = D - A_{sym} \quad (10)$$

260 Where D is the degree matrix of A_{sym} with $D_{ii} = \sum_j (A_{sym})_{ij}$. This construction allows CTQW
 261 trainable and to be trained jointly with downstream tasks.

262 Given the learned Hamiltonian, we consider an initial state set consisting of orthonormal basis states,
 263 represented by the identity matrix I_n , where each column corresponds to an initial state concentrated
 264 on a single node, and a set of time steps $\mathcal{T} = \{1, 2, \dots, T\}$. Subsequently, we can simulate the
 265 state evolution of CTQW under various configurations using Schrödinger equation. By stacking the
 266 probability distribution under n single-node initial states over T distinct time steps, we obtain the
 267 temporal evolution tensor $P \in R^{T \times n \times n}$, which capture the temporal dynamics of the graph. The
 268 tensor provides a rich and physically grounded representation of the graph, and thus can be used in
 269 downstream models such as graph Transformers and recurrent network for graph-level tasks.

270 3.3 THE QUANTUM WALK-GRAPH TRANSFORMER MODULE
271

272 Although graph Transformers offer a global receptive field that enables comprehensive message
273 passing among all nodes, the self-attention mechanism primarily captures semantic similarity and
274 often neglects the inherent structure properties. To compensate for this, we design The Quantum
275 Walk-Graph Transformer to integrate structural prior information derived from CTQW into the at-
276 tention mechanism, enabling the model to account for both semantic and structural relations between
277 nodes. Specifically, we utilize the final-time transition probabilities $P^T \in \mathbb{R}^{n \times n}$ from CTQW as
278 a static structural bias matrix, which is normalized and log-scaled before being added to the self-
279 attention score matrix.

280
$$\text{Attention}(Q, K, V, B) = \text{softmax}\left(\frac{QK^T}{\sqrt{d}} + B\right)V \quad (11)$$

281
282

283 Where $Q = XW^Q, K = XW^K, V = XW^V$ are the projected query, key and value matrices.
284 The structural bias B is derived from CTQW probability matrix $P^T \in \mathbb{R}^{n \times n}$ at final time step
285 T . To ensure stability, P^T is column-normalized into a stochastic matrix and then transformed as
286 $B = \log(1 + P^T)$. Then node representation is updated and aggregated to produce the CTQW-based
287 graph-level representation O_{QWGT} . By integrating the inherent physically grounded structural bias
288 into the attention mechanism, the model gains a richer understanding of graph topology beyond pure
289 node feature similarity.

290 3.4 THE QUANTUM WALK-GRAPH RECURRENT MODULE
291

292 In contrast to the convergence behavior of classical random walks, the evolution of quantum walks is
293 dynamic and oscillatory. These fluctuations encode rich temporal and structural patterns that cannot
294 be captured by static structural bias alone. To model the dynamic evolution of quantum states, we
295 design The Quantum Walk-Graph Recurrent Module, which processes the full CTQW probability
296 sequence over multiple time steps.

297 We treat the temporal evolution tensor $P \in \mathbb{R}^{T \times n \times n}$, generated by evolving each of n single-node
298 initial states over T discrete time steps, as a temporal input tensor. We extract probability matrix
299 for each single-node initial state $|i\rangle$ over T discrete time steps $P_i = [P_i^1, P_i^2, \dots, P_i^T] \in \mathbb{R}^{n \times n}$,
300 Where P_i^t denotes the probability distribution of CTQW under initial state $|\psi(0)\rangle = |i\rangle$ at time t .
301 The sequence is first transformed into a hidden representation via a linear layer and then fed into a
302 BiGRU to model the temporal evolution and fluctuations of each node, enabling the model to capture
303 complex temporal dependencies in both forward and backward directions.

304
$$H_{GRU} = \text{BiGRU}(\text{Linear}(P_i)) \quad (12)$$

305

306 These resulting node representations are aggregated using mean pooling and followed by a feedfor-
307 ward network to generate graph-level representation O_{QWGR} .

308
$$O_{QWGR} = \text{FFN}(\text{MeanPool}(H_{GRU})) \quad (13)$$

309

310 This module effectively models the dynamic evolution of CTQW, providing a complementary per-
311 spective to the static structural view offered by the QWGT module.

312 3.5 FUSION AND PREDICTION
313

314 we construct the CTQWformer layer by integrating the QWGT module and the QWGR module.
315 The QWGT module generates graph-level representations by leveraging CTQW-based structural
316 biases through attention mechanism in the graph Transformer, while the QWGR module extracts
317 graph-level embeddings from the temporal evolution tensor using a BiGRU network. The outputs
318 from these two modules are concatenated and passed through a feed-forward fusion network to
319 produce a unified representation. By stacking multiple CTQWformer layer, the model progressively
320 refines graph representations. At each layer, the graph-level embedding is broadcast back to node-
321 level representations to guide subsequent layers. The final node embeddings from the last layer are
322 aggregated via global mean pooling operation to obtain the final graph-level representation and then
323 fed into a multi-layer classifier for prediction.

Dataset	MUTAG	PTC(MR)	PROTEINS	DD	IMDB-B	IMDB-M
# Graphs	188	344	1113	1178	1000	1500
# Classes	2	2	2	2	2	3
Max # Vertices	28	109	620	5748	136	89
Mean # Vertices	17.93	14.29	39.06	284.32	19.77	13.00
# Node Features	7	18	3	89	0	0
Description	Bio	Bio	Bio	Bio	SN	SN

Table 1: Statistics of benchmark graph datasets.

Model	MUTAG	PTC(MR)	PROTEINS	DD	IMDB-B	IMDB-M
GCGK	81.58 \pm 2.11	57.26 \pm 1.41	71.67 \pm 0.55	78.45 \pm 0.26	65.87 \pm 0.98	43.89 \pm 0.38
WLSK	82.05 \pm 0.36	57.97 \pm 0.49	74.68 \pm 0.49	79.78 \pm 0.36	73.40 \pm 4.63	49.33 \pm 4.75
JTQK	85.50 \pm 0.55	58.50 \pm 0.39	–	79.89 \pm 0.32	–	–
QJSK	82.72 \pm 0.44	56.70 \pm 0.49	70.13 \pm 4.88	77.68 \pm 0.31	62.10	43.24
HAQJSK	85.83 \pm 0.72	62.35 \pm 0.51	–	–	73.50 \pm 0.45	50.08\pm0.20
AERK	88.55 \pm 0.43	59.38 \pm 0.36	–	77.60 \pm 0.47	–	–
CTQWformer	92.54\pm5.39	69.16\pm5.17	78.53\pm2.34	81.24\pm3.43	76.40\pm1.91	47.47 \pm 7.84

Table 2: Graph classification results (% \pm standard deviation) comparing with graph kernel methods. Best scores are in bold.

4 EXPERIMENTS

We conduct extensive experiments for graph classification on several benchmark datasets from the TU collection Morris et al. (2020), covering domains including bioinformatics (Bio) and social networks (SN). The detailed statistical information of these datasets is summarized in Table 1. To ensure that all datasets have meaningful node features, we preprocess the graphs by appending normalized node degree using log-scaled max normalization to existing features if available, or using it as the sole node feature otherwise. This approach is commonly adopted in GNN literature You et al. (2020) to enrich structural information in datasets lacking node features such as IMDB-B, IMDB-M Yanardag & Vishwanathan (2015). To evaluate the performance of our proposed CTQWformer, we compare it with two major categories of baseline methods: (1) graph kernel methods and (2) graph neural network approaches.

4.1 COMPARISONS WITH GRAPH KERNEL METHODS

Baseline and Experimental Settings. We compare the proposed CTQWformer with six graph kernels, including two classical R-convolution graph kernels, (1) the Graphlet Count Graph Kernel (GCGK) Shervashidze et al. (2009) and (2) the Weisfeiler-Lehman Subtree Kernel (WLSK) Shervashidze et al. (2011); four information-theoretic graph kernels, (3) Jensen-Tsallis q-difference Kernel (JTQK) Bai et al. (2014), (4) Quantum Jensen-Shannon Kernel (QJSK) Bai et al. (2015), (5) Hierarchical-Aligned Quantum Jensen-Shannon Kernels (HAQJSK) Bai et al. (2024), (6) Aligned Entropic Reproducing Kernels (AERK) Cui et al. (2023). Notably, all four of these information-theoretic graph kernels are built upon CTQW, demonstrating the potential of CTQW for graph learning. However, the inherent limitations of kernel-based methods prevent them from fully leveraging the rich dynamical evolution information generated by CTQW on graphs.

Experimental Results and Analysis. As shown in Table 2, CTQWformer consistently outperforms existing kernel-based methods, including both R-convolution graph kernels and CTQW-based graph kernels, demonstrating its superior ability in capturing graph-level representations. In particular, CTQWformer achieves the best performance on five out of six datasets, except for IMDB-M. This may result from the lack of sufficiently informative node features. While prior CTQW-based kernels already demonstrated the potential of CTQW for graph learning, their performance is limited by the inherent nature of kernel methods. In contrast, CTQWformer integrates the dynamical evolution of CTQW into a trainable representation learning framework, enabling the model to effectively leverage temporal evolution information of CTQW. These results validate the effectiveness of integrating graph neural networks with the dynamical information derived from CTQW on graphs, enabling the model to better capture and exploit the dynamics information of CTQW for graph learning.

Model	MUTAG	PTC(MR)	PROTEINS	DD	IMDB-B	IMDB-M
GIN-0	89.40 \pm 5.60	64.60 \pm 7.00	76.20 \pm 2.80	—	75.10 \pm 5.10	52.30\pm2.80
DGCNN	85.83 \pm 1.66	58.59 \pm 2.47	75.54 \pm 0.94	79.37 \pm 0.94	70.03 \pm 0.86	47.83 \pm 0.85
PSCN	88.95 \pm 4.37	62.29 \pm 5.68	75.00 \pm 2.51	76.27 \pm 2.64	71.00 \pm 2.29	45.23 \pm 2.84
GAT	89.40 \pm 6.10	66.70 \pm 5.10	74.70 \pm 2.20	—	70.50 \pm 2.30	47.80 \pm 3.10
GCN	87.20 \pm 5.11	62.10 \pm 1.80	75.65 \pm 3.24	79.12 \pm 3.07	73.30 \pm 5.29	51.20 \pm 5.13
CAPSGNN	86.67 \pm 6.88	66.01 \pm 5.91	76.40 \pm 4.17	77.62 \pm 4.99	71.69 \pm 3.40	48.50 \pm 4.10
GraphSAGE	79.80 \pm 13.9	63.90 \pm 7.70	65.90 \pm 2.70	65.80 \pm 4.90	72.40 \pm 3.60	49.90 \pm 5.00
CTQWformer	92.54\pm5.39	69.16\pm5.17	78.53\pm2.34	81.24\pm3.43	76.40\pm1.91	47.47 \pm 7.84

Table 3: Graph classification results (% \pm standard deviation) comparing with GNN-based methods. Best scores are in bold.

4.2 COMPARISONS WITH GNN APPROACHES

Baseline and Experimental Settings. We compare CTQWformer against seven GNN approaches. The GNN-based baselines consist of (1) Graph Isomorphism Network (GIN-0) Xu et al. (2018), (2) Deep Graph Convolutional Neural (DGCNN) Zhang et al. (2018a), (3) PATCHY-SAN Convolutional Neural Network (PSCN) Niepert et al. (2016), (4) Graph Attention Network (GAT) Veličković et al. (2017), (5) Graph Convolutional Network (GCN) Kipf & Welling (2016), (6) Capsule Graph Neural Network (CAPSGNN) Xinyi & Chen (2018), and (7) Graph Sample and Aggregation (GraphSAGE) Hamilton et al. (2017). These baselines encompass convolutional, attention-based, sorting-based, and capsule-based GNN models, providing a comprehensive comparison with our proposed quantum walk-inspired framework. We follow the standard 10-fold cross-validation setting for all datasets, where accuracy is reported as the mean and standard deviation over 10 folds. Unless otherwise specified, we set the number of CTQWformer layer to 2, and the time steps to 4, the hidden dimension is fixed to 64, and dropout is set to 0.3. We use Adam optimizer with a learning rate of 0.001. And train model for 300 epochs with early stop technique, we slightly adjust the number of layers and time steps to obtain the best performance, within a small grid search range. For baseline methods, we adopt the results reported from their original papers or widely used benchmark studies in published papers Nguyen et al. (2022); Zhang et al. (2018b) for fair comparison.

Experimental Results and Analysis. Table 3 shows that CTQWformer achieves the best or highly competitive performance across all datasets except IMDB-M. A potential reason is that the dataset does not provide original node features and consists of relatively small graphs, making it challenging for models like CTQWformer that rely on meaningful node feature information. Nevertheless, the results clearly indicate that CTQWformer successfully integrates CTQW into GNN approaches, providing consistent improvements over conventional GNN baselines. These results demonstrate the effectiveness of incorporating CTQW-based structural priors and temporal information into a trainable deep learning architecture. Unlike traditional GNNs that rely on local message passing, CTQWformer benefits from a global structural perspective via dynamical evolution of CTQW on graphs, which allows the model to better capture complex topological and effectively incorporate node features in graphs.

4.3 THE FURTHER ANALYSIS FOR CTQWFORMER

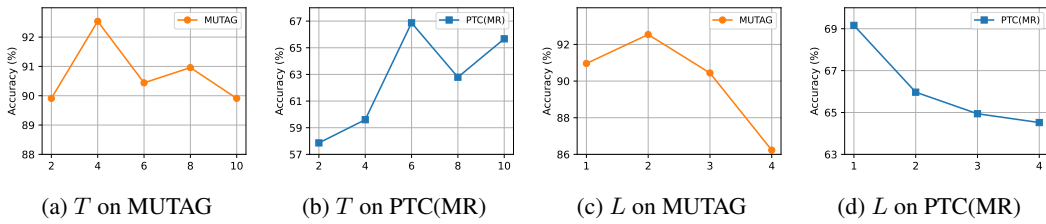
Model	MUTAG	PTC(MR)	PROTEINS
CTQWformer	92.54\pm5.39	69.16\pm5.17	78.53\pm2.34
w/o QWGT	89.39 \pm 5.74	59.62 \pm 4.87	77.72 \pm 2.41
w/o QWGR	74.97 \pm 7.17	57.87 \pm 3.25	69.00 \pm 5.49

Table 4: Ablation study of CTQWformer on three datasets.

Ablation Study. To assess the contribution of each module in CTQWformer, we perform ablation studies by removing the QWGT module and the QWGR module respectively. The results are reported in Table 4. As shown in the table, we find that removing the QWGR module leads to a significant performance drop across all three test datasets, with accuracy on MUTAG, for instance, decreasing from 92.54% to 74.97%. This highlights the critical importance of modeling dynamical evolution of CTQW to learn graph representations. In contrast, removing the QWGT module results

432 in a small performance decrease, indicating that while CTQW-based structural bias contributes positively, it plays a less dominant role compared to temporal evolution modeling. Meanwhile, we also observe relatively large standard deviations in some cases, which may be attributed to the inherent dynamics and fluctuation of CTQW evolution, further investigation into these properties remains an important direction for future work.

437 **Hyperparameter Analysis.** We further investigate the sensitivity of key hyperparameters of
438 CTQWformer, focusing on both the time steps of CTQW and the network depth of the model.



440
441 Figure 2: Sensitivity analysis of time steps T and network depth L .

442 **Time Steps in CTQW.** Since the dynamics of CTQW is adaptively guided by the learned Hamiltonian,
443 and simulated by traversing all single-node initial states on the graph. We vary the number
444 of time steps $T \in \{2, 4, 6, 8, 10\}$ to study the model’s sensitivity to the temporal granularity of
445 CTQW on MUTAG and PTC(MR) datasets. We observe that the classification accuracy on the
446 MUTAG dataset increases with the number of time steps at first and reaches its peak at time steps
447 $T = 4$ (92.54%), indicating that moderate evolution time in CTQW captures informative structural
448 patterns. However, further increasing the time steps leads to a decline in performance, likely due
449 to quantum interference effects or over-smoothing, suggesting that an overly long CTQW evolution
450 may dilute discriminative information. While on the PTC(MR) dataset, increasing time steps from 2
451 to 6 improves accuracy significantly, indicating better temporal evolution feature capture. Beyond 6
452 steps, accuracy fluctuates and slightly drops, suggesting excessive steps may introduce redundancy.
453 Thus, 6 time steps offer the best balance between performance and complexity.

454 **Number of Layers in CTQWformer.** Besides, We vary the number of stacked CTQWformer
455 layers $L \in \{1, 2, 3, 4\}$ to study the effect of network depth. As shown in Figure 3, On MUTAG
456 dataset, the model achieves the highest accuracy with a 2-layer network, outperforming shallower
457 and deeper configurations. This suggests that moderate depth balances representation power and
458 training stability, while excessive depth may cause overfitting or optimization difficulties. While on
459 PTC(MR) dataset, accuracy consistently decreases as the network depth increases from 1 layer to
460 4 layers, indicating that deeper networks may lead to over-smoothing or overfitting on this smaller
461 datasets, where node representations become indistinguishable and less informative. Overall, these
462 findings highlight the critical importance of judiciously configuring model depth in alignment with
463 the structural complexity and scale of datasets. Empirical evidence from both datasets indicates that
464 a moderate network depth offers a favorable trade-off between expressiveness and generalization,
465 while overly deep architectures tend to diminish performance, particularly in scenarios involving
466 smaller graphs.

5 CONCLUSION

467 In this paper, we have proposed CTQWformer, a novel CTQW-based Transformer model for graph
468 classification task. Our model realizes trainable CTQW on graphs by integrating both graph struc-
469 ture and node features into a learnable Hamiltonian, enabling the model to capture rich and intricate
470 graph structure information. Furthermore, the model incorporates a graph Transformer and a re-
471 current neural network, which are respectively designed to leverage static physical structural bias
472 and dynamic temporal evolution patterns derived from CTQW. Extensive experiments on multiple
473 benchmark datasets demonstrate the effectiveness and superiority of our method, highlighting the
474 potential of integrating quantum walk dynamics with graph neural networks for graph learning.

486 REPRODUCIBILITY STATEMENT
487488 We have made significant efforts to ensure the reproducibility of our results. The full implementation
489 of CTQWformer, along with data preprocessing scripts and instructions for running the experiments,
490 is provided in the supplementary materials.
491492 REFERENCES
493494 Dorit Aharonov, Andris Ambainis, Julia Kempe, and Umesh Vazirani. Quantum walks on graphs.
495 In *Proceedings of the thirty-third annual ACM symposium on Theory of computing*, pp. 50–59,
496 2001.497 Lu Bai, Luca Rossi, Horst Bunke, and Edwin R Hancock. Attributed graph kernels using the jensen-
498 tsallis q-differences. In *Joint European Conference on Machine Learning and Knowledge Dis-*
499 *covery in Databases*, pp. 99–114. Springer, 2014.
500501 Lu Bai, Luca Rossi, Andrea Torsello, and Edwin R Hancock. A quantum jensen–shannon graph
502 kernel for unattributed graphs. *Pattern Recognition*, 48(2):344–355, 2015.
503504 Lu Bai, Lixin Cui, Yue Wang, Ming Li, Jing Li, Philip S Yu, and Edwin R Hancock. Haqsk:
505 Hierarchical-aligned quantum jensen–shannon kernels for graph classification. *IEEE Transactions*
506 *on Knowledge and Data Engineering*, 36(11):6370–6384, 2024.507 Gabriele Corso, Hannes Stark, Stefanie Jegelka, Tommi Jaakkola, and Regina Barzilay. Graph
508 neural networks. *Nature Reviews Methods Primers*, 4(1):17, 2024.
509510 Lixin Cui, Ming Li, Yue Wang, Lu Bai, and Edwin R Hancock. Aerk: Aligned entropic reproducing
511 kernels through continuous-time quantum walks. *arXiv preprint arXiv:2303.03396*, 2023.512 Mark Goldsmith, Harto Saarinen, Guillermo García-Pérez, Joonas Malmi, Matteo AC Rossi, and
513 Sabrina Maniscalco. Link prediction with continuous-time classical and quantum walks. *Entropy*,
514 25(5):730, 2023.
515516 Will Hamilton, Zhitao Ying, and Jure Leskovec. Inductive representation learning on large graphs.
517 *Advances in neural information processing systems*, 30, 2017.518 David Haussler et al. Convolution kernels on discrete structures. Technical report, Technical report,
519 Department of Computer Science, University of California . . . , 1999.
520521 Karuna Kadian, Sunita Garhwal, and Ajay Kumar. Quantum walk and its application domains: A
522 systematic review. *Computer Science Review*, 41:100419, 2021.
523524 Thomas N Kipf and Max Welling. Semi-supervised classification with graph convolutional net-
525 works. *arXiv preprint arXiv:1609.02907*, 2016.526 Nils M Kriege, Fredrik D Johansson, and Christopher Morris. A survey on graph kernels. *Applied*
527 *Network Science*, 5(1):6, 2020.
528529 Christopher Morris, Nils M Kriege, Franka Bause, Kristian Kersting, Petra Mutzel, and Marion
530 Neumann. Tudataset: A collection of benchmark datasets for learning with graphs. *arXiv preprint*
531 *arXiv:2007.08663*, 2020.532 Dai Quoc Nguyen, Tu Dinh Nguyen, and Dinh Phung. Universal graph transformer self-attention
533 networks. In *Companion Proceedings of the Web Conference 2022*, pp. 193–196, 2022.
534535 Mathias Niepert, Mohamed Ahmed, and Konstantin Kutzkov. Learning convolutional neural net-
536 works for graphs. In *International conference on machine learning*, pp. 2014–2023. PMLR, 2016.
537538 Ladislav Rampášek, Michael Galkin, Vijay Prakash Dwivedi, Anh Tuan Luu, Guy Wolf, and Do-
539 minique Beaini. Recipe for a general, powerful, scalable graph transformer. *Advances in Neural*
Information Processing Systems, 35:14501–14515, 2022.

540 Nino Shervashidze, SVN Vishwanathan, Tobias Petri, Kurt Mehlhorn, and Karsten Borgwardt. Efficient
 541 graphlet kernels for large graph comparison. In *Artificial intelligence and statistics*, pp.
 542 488–495. PMLR, 2009.

543 Nino Shervashidze, Pascal Schweitzer, Erik Jan Van Leeuwen, Kurt Mehlhorn, and Karsten M Borg-
 544 wardt. Weisfeiler-lehman graph kernels. *Journal of Machine Learning Research*, 12(9), 2011.

545 Ashish Vaswani, Noam Shazeer, Niki Parmar, Jakob Uszkoreit, Llion Jones, Aidan N Gomez,
 546 Łukasz Kaiser, and Illia Polosukhin. Attention is all you need. *Advances in neural informa-
 547 tion processing systems*, 30, 2017.

548 Petar Veličković, Guillem Cucurull, Arantxa Casanova, Adriana Romero, Pietro Lio, and Yoshua
 549 Bengio. Graph attention networks. *arXiv preprint arXiv:1710.10903*, 2017.

550 Zonghan Wu, Shirui Pan, Fengwen Chen, Guodong Long, Chengqi Zhang, and Philip S Yu. A
 551 comprehensive survey on graph neural networks. *IEEE transactions on neural networks and
 552 learning systems*, 32(1):4–24, 2020.

553 Zhang Xinyi and Lihui Chen. Capsule graph neural network. In *International conference on learning
 554 representations*, 2018.

555 Keyulu Xu, Weihua Hu, Jure Leskovec, and Stefanie Jegelka. How powerful are graph neural
 556 networks? *arXiv preprint arXiv:1810.00826*, 2018.

557 Ge Yan, Yehui Tang, and Junchi Yan. Towards a native quantum paradigm for graph representation
 558 learning: A sampling-based recurrent embedding approach. In *Proceedings of the 28th ACM
 559 SIGKDD Conference on Knowledge Discovery and Data Mining*, pp. 2160–2168, 2022.

560 Pinar Yanardag and SVN Vishwanathan. Deep graph kernels. In *Proceedings of the 21th ACM
 561 SIGKDD international conference on knowledge discovery and data mining*, pp. 1365–1374,
 562 2015.

563 Chengxuan Ying, Tianle Cai, Shengjie Luo, Shuxin Zheng, Guolin Ke, Di He, Yanming Shen, and
 564 Tie-Yan Liu. Do transformers really perform badly for graph representation? *Advances in neural
 565 information processing systems*, 34:28877–28888, 2021.

566 Jiaxuan You, Zhitao Ying, and Jure Leskovec. Design space for graph neural networks. *Advances
 567 in Neural Information Processing Systems*, 33:17009–17021, 2020.

568 Lei Yu, Hongyang Chen, Jingsong Lv, and Linyao Yang. Gqwformer: A quantum-based transformer
 569 for graph representation learning. *arXiv preprint arXiv:2412.02285*, 2024.

570 Seongjun Yun, Minbyul Jeong, Raehyun Kim, Jaewoo Kang, and Hyunwoo J Kim. Graph trans-
 571 former networks. *Advances in neural information processing systems*, 32, 2019.

572 Muhan Zhang, Zhicheng Cui, Marion Neumann, and Yixin Chen. An end-to-end deep learning
 573 architecture for graph classification. In *Proceedings of the AAAI conference on artificial intelli-
 574 gence*, volume 32, 2018a.

575 Yi Zhang, Lulu Wang, and Liandong Wang. A comprehensive evaluation of graph kernels for
 576 unattributed graphs. *Entropy*, 20:984, 2018b.

577
 578
 579
 580
 581
 582
 583
 584
 585
 586
 587
 588
 589
 590
 591
 592
 593

594 **A COMPLEXITY ANALYZE OF CTQWFORMER**
 595

596 We analyze the computational and memory costs of the core CTQW computations used in CTQW-
 597 former and summarize practical trade-offs for scaling.
 598

599 **Exact matrix-exponential.** Given a graph with n nodes and a Hamiltonian $H \in \mathbb{R}^{n \times n}$, computing
 600 the matrix exponential $U(t) = \exp^{-iHt}$ by direct dense methods (e.g., scaling-and-squaring + Padé)
 601 requires $\mathcal{O}(n^3)$ time and $\mathcal{O}(n^2)$ memory per time step. If we compute $U(t)$ at T distinct time points
 602 independently, the worst-case time complexity is

603 $\text{Time}_{\text{dense}} = \mathcal{O}(T \cdot n^3), \quad \text{Space}_{\text{dense}} = \mathcal{O}(n^2),$
 604

605 and then we store the full evolution tensor $P \in \mathbb{R}^{T \times n \times n}$ the space grows to $\mathcal{O}(T \cdot n^2)$.
 606

607 **Memory trade-offs and what to store.** CTQWformer uses CTQW-derived information in two
 608 ways: (i) the final-time structural bias P_T for the Graph Transformer module, and (ii) temporal
 609 sequences for the Graph recurrent module. Storing the full pairwise evolution tensor $P \in \mathbb{R}^{T \times n \times n}$
 610 is often the dominant memory cost ($\mathcal{O}(Tn^2)$).
 611

612 **Structural Bias of CTQW in The QWGT module** Specifically, given the raw transition proba-
 613 bility matrix P^T with entries p_{ij}^T , we normalize along the column dimension to obtain a stochastic
 614 matrix

615
$$\tilde{P}_{ij}^T = \frac{p_{ij}^T}{\sum_{i'} p_{i'j}^T}, \quad (14)$$

 616

617 ensuring that $\sum_i \tilde{P}_{ij}^T = 1$ for each j . The structural bias is then defined as
 618

619
$$B = \log(1 + \tilde{P}^T), \quad (15)$$

 620

621 which stabilizes training and smooths the influence of CTQW probabilities when added to the atten-
 622 tion logits.
 623

624 **Temporal Sequence of CTQW in the QWGR module** In addition to the final-time distribution,
 625 we also leverage the temporal evolution information of CTQW. The temporal evulution tensor P is
 626 treated as a sequence input, where $P^t \in \mathbb{R}^{N \times N}$.
 627

628 For each node i , we extract its temporal sequence from the diagonal entries of P^t :

629
$$s_i = \{p_{ii}^t\}_{t=1}^T, \quad (16)$$

 630

631 where p_{ii}^t denotes the probability that the walker remains at node i at time step t . These node-level
 632 time series are projected into a latent space and then fed into a bidirectional GRU (BiGRU) encoder:
 633

634
$$h_i = \text{BiGRU}(s_i), \quad (17)$$

 635

636 where h_i is the middle representation of hidden layer capturing both forward and backward temporal
 637 dependencies of node i . The resulting node embeddings $\{h_i\}_{i=1}^N$ are aggregated by mean pooling:
 638

639
$$h_G = \frac{1}{N} \sum_{i=1}^N h_i, \quad (18)$$

 640

641 and further transformed by a feed-forward readout network to obtain the final graph-level embed-
 642 ding.
 643

644 **Fusion Strategy.** Finally, the two branches operate in parallel and produce graph-level vectors:
 645 O_{QWGT} from the QWGT module and O_{QWGR} from the QWGR module. They are fused by concate-
 646 nation:
 647

$$O_{\text{fused}} = [O_{\text{QWGT}} \parallel O_{\text{QWGR}}],$$

648 The fused representation is then passed through a feed-forward projection to form the final graph
 649 embedding used for classification.
 650

648 B NUMERICAL SIMULATION OF CONTINUOUS-TIME QUANTUM WALK
649650 For the numerical simulations of CTQWs, we utilize PyTorch for the matrix exponential computa-
651 tions, running on an RTX 4090 GPU, with a CPU configuration of 16-core Intel(R) Xeon(R) Gold
652 6430 and 120GB RAM. Additional implementation and training details can be found in the supple-
653 mentary materials.654 It is worth noting that under the scale of the benchmark datasets used in this work, directly com-
655 puting the evolution operator $U(t) = e^{-iHt}$ is feasible with current hardware, and the numeri-
656 cal stability is well maintained. More importantly, the design of CTQWformer is not restricted to
657 small graphs. In our implementation, the matrix exponential e^{-iHt} is computed using PyTorch's
658 built-in `torch.matrix_exp`, which internally relies on a scaling-and-squaring with Padé approxi-
659 mation method. This ensures differentiability and compatibility with automatic back-propagation.
660 For small to medium-scale benchmarks, we adopt the exact matrix exponential to minimize numeri-
661 cal approximation errors and provide a clean evaluation of the model itself. For larger graphs, these
662 approximations can be seamlessly integrated without altering the framework. In fact, the model only
663 requires applying $U(t)$ to vectors (i.e., computing $U(t)v$), which can be efficiently approximated on
664 large graphs using Krylov subspace or Lanczos methods without explicitly forming the full matrix
665 exponential. Such approximations scale similarly to sparse matrix–vector multiplications, making
666 them applicable to graphs with tens of thousands of nodes or more. Therefore, while our exper-
667 iments focus on small- to medium-scale graphs, CTQWformer is inherently scalable and can be
668 naturally extended to large-scale graph learning tasks.
669670 C ON THE COMPARISON WITH GRAPH TRANSFORMERS
671672 We note that graph Transformer architectures such as Graphomer Ying et al. (2021) and GraphGPS
673 Rampášek et al. (2022). Graphomer enhances Transformer for graphs via integrating structural bi-
674 ases and centrality encoding, while GraphGPS unifies local, global and relative attention to capture
675 multi-scale graph structure information. They are primarily designed for large-scale datasets (e.g.,
676 OGB benchmarks), and their scalability and structural encodings show advantages. However, re-
677 producing their results on TU collection datasets is non-trivial, as their original implementations are
678 not tailored for small-scale graph classification tasks and often require heavy hyperparameter tuning
679 to yield stable results. More importantly, our CTQWformer is not a pure graph Transformer: it is
680 a hybrid framework that integrates quantum walk dynamics with graph Transformers and recurrent
681 network, thereby providing complementary modeling of temporal evolution beyond the structural
682 biases used in Graphomer/GraphGPS. We therefore regard these models as orthogonal to our con-
683 tribution, and leave extensive large-scale comparisons to future work.
684685 D THE USAGE DISCLOSURE OF LARGE LANGUAGE MODELS
686687 We used large language models (LLMs), specifically ChatGPT and Deepseek, as assistive tools
688 during the preparation of this paper. The LLM was employed only for language refinement and
689 improving readability, such as rephrasing sentences, polishing grammar, and adjusting writing style,
690 and for code debugging support in the experiments. All research ideas, model design, theoretical
691 analysis, and experimental implementation were conceived and carried out solely by the authors.
692 The LLM did not contribute to the development of research methodology, experimental setup, or
693 interpretation of results. The authors take full responsibility for the content of this paper.
694
695
696
697
698
699
700
701